International Journal of Industrial Electronics, Control and Optimization © 2019 IECO
Vol. 2, No. 2, pp. 127-136, April (2019)

Sliding Mode Control of LLC Resonant DC-DC Converter for Wide Output Voltage Range in Battery Charging

Asghar Taheri[†1], Nader Asgari[2]

[1,2] Department of Electrical Engineering, University of Zanjan, Zanjan, Iran.

ABSTRACT

In this paper, a sliding mode control of the LLC resonant dc-dc converter low voltage and high current to the battery charger for electric vehicles is presented. The proposed controller operates at two fixed switching frequencies with sliding mode control implementation. In resonant converter, because of the soft-switching process, switching loss is negligible and converters can be designed at high frequencies to decline their size, weight and price. To analyze this convertor the harmonic approximation method with state space equation is used. Taking advantage of the approximations used in order to avoid uncertainty, sliding mode control method is used. The mentioned convertor with the proposed controlled is exploited within three switching frequency bands that are lower than resonant frequency, resonant frequency and above resonant frequency. Due to the robustness of the sliding mode control, the output voltage regulation occurs with minimum distortion under a wide variation of input voltage, output voltage and output current. As a result, the battery life increases. In order to verify the results and effectiveness of the proposed converters, the prototype of LLC resonant converters Simulation and experimental results for the input voltage (300-420Vdc), output voltage (36-72Vdc) and current output (0-11A) is presented. The prototype achieves a peak efficiency value of 96%.

Article Info

Keywords:
Batteries, Electric Vehicles (EV),
LLC Resonant Converter, Sliding Mod Control (SMC),
Zero Voltage Switching (ZVS).

Article History:
Received 2018-10-19
Accepted 2018-12-28

I. INTRODUCTION

Electric Vehicles (EVs) are propelled by an electric motor that is supplied with power from are the chargeable battery [1-2]. Presently, the performance characteristics required for many electric vehicle (EV) applications far exceed the storage capabilities of conventional battery systems. However, battery technology is improving and as this transition occurs, the charging of these batteries becomes very complicated due to the high voltages and currents involved in the system and the sophisticated charging algorithms [3]. Quick charging of high capacity battery packs causes increased disturbances in the ac utility power system, thereby increasing the need for efficient, low-distortion smart chargers[4].

The battery charger can respond to the condition of a battery and modify its charging actions according to the battery algorithm. Conversely, a standard or simple battery charger supplies a constant dc or pulsed dc power source to a battery being charged. A simple charger does not alter its output based on time or the charge on the battery. Therefore, smart chargers are preferred for EV battery charging applications. The proposed EV battery charger power architecture includes an ac–dc converter with power factor correction (PFC) [5-6], followed by an isolated dc–dc converter, as shown in Fig . 1. [6]. This architecture virtually eliminates the low- and high frequency current ripple charging the battery without using a bulky filter capacitor. Instead, it uses a high-frequency transformer. This structure maximizes battery life time without penalizing the charger volume. In the work that follows, the front-end ac–dc PFC converter is a conventional continuous conduction mode (CCM) boost topology [7-8]. Second stage of dc–dc converter is a half-bridge resonant LLC converter. The criteria for choosing these topologies include high reliability, high efficiency, and low component cost.

[1]**Corresponding Author** : taheri@znu.ac.ir
Tel: +982433054066
[1] Department of Electrical Engineering, University of Zanjan
[2] University of Zanjan

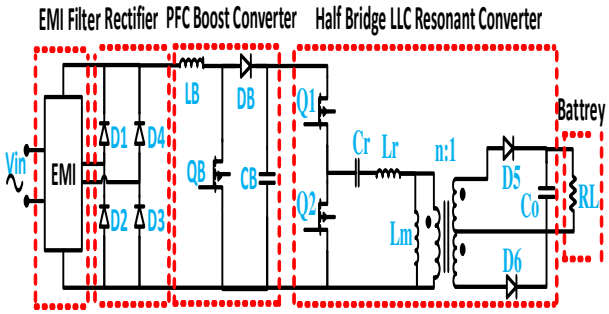


Fig. 1. Typical battery charging power architecture.

The half-bridge resonant LLC converter is widely used in the telecom industry for its high efficiency at the resonant frequency and its ability to regulate the output voltage during the hold-up time, where the output voltage is constant and the input voltage might drop significantly [8]. Resonant converters have been used in many applications, including induction heating [9], and fuel cells [10]. However, the wide output voltage range requirements for a battery charger are drastically different and challenging compared to telecom applications, which operate in a narrow output voltage range. Fig. 2 illustrates a simplified battery charging profile. It has four distinct operating modes: bulk, absorption, equalization, and maintenance. In the bulk mode, the charger limits the maximum charging current to a preset I_{max} value while monitoring the battery voltage. In the absorption mode, the charger elevates the voltage to V_{ABS} while monitoring the current. This voltage is just below the battery gassing voltage. When it has reached this point, the battery is between 70% and 90% State Of Charge (SOC). When the current decreases to a preset value, I_{min}, the charger enters the equalization mode. When it has reached this point, the battery is at 100% SOC. Equalizing is an overcharge performed on batteries after they have been fully charged. This function equalizes the cell voltages in a battery module. In the maintenance mode, the charging action is finished and the charger only supplies limited current to offset the internal soft discharge. Fig. 2, shows simplified adaptive 4-step lead acid battery charging profile. As indicated in Fig. 2, the battery voltage, at the dc–dc converter output, can vary from V_{min} to V_{max}. Therefore, the design requirements for selecting the resonant tank components are significantly different than those in telecom applications featuring a constant output voltage [3]. The authors in [11-13] addressed wide output range applications; however, the design procedures are given for resonant tank components using the first harmonic approximation proposed in [14]-[17] which is only valid for frequencies close to the resonant frequencies. According to the characteristics of the batteries used in electric vehicles, Fig. 2, shows a wide range of voltage with different currents for a battery charger are needed. For this purpose, LLC resonant converters can achieve both high efficiency and wide input voltage and output voltage capability because of its voltage gain characteristics and small switching loss. However, the efficiency of LLC resonant converter still cannot meet the recent efficiency target from industry [3]. Achieving ZVS is another design for reducing

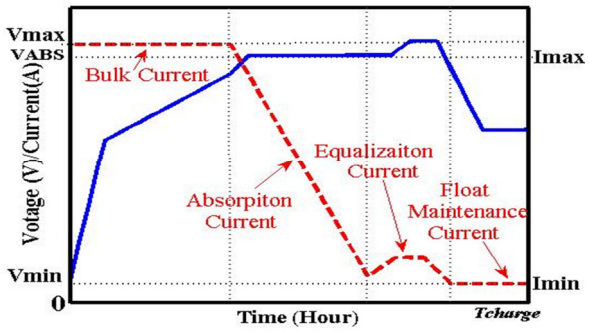


Fig. 2.Simplified adaptive 4-step lead acid battery charging profile.

Electromagnetic Interference (EMI) and switching losses, especially under the light load conditions [14]. Following a proper design procedure, LLC resonant converter can realize narrow switching frequency range according to the input voltage and the load current, ZVS of primary switches [20] However, due to the pulse frequency modulation, it is difficult to achieve outstanding performance in the dynamic response. Also, it is difficult to design the closed-loop control parameters, because dynamics of LLC resonant converter varies significantly as the operation conditions [15-16]. Sliding mode control has been widely and successfully applied in both nonlinear and linear systems [18-20]. It is well-known for its strong robustness against parameter uncertainties and load variation, together with the fast transient response and strong anti-interference [21]. The main drawback of sliding mode control is the chattering phenomenon which consists of the oscillation of the control signal [22].

In this paper, a sliding-mode control of LLC resonant dc-dc converter with low voltage and high current to the battery charger for electric vehicles is presented. This method is different from the conventional PFM control. The closed-loop regulation of output voltage for charging battery can be achieved by changing switching frequency between two fixed values. Proposed control is robust in wide variation of input voltage, output voltage and output current. In order to improving converter efficiency, the operation of LLC resonant converter is fixed at two specific switching frequencies with a sliding mode control implementation. The sliding surface consists of output voltage error and the output filter capacitor current. SMC has a very fast transient response to load variation. Also, it is well known for its strong robustness against parameter uncertainties in the analysis of the dynamical nonlinear equations. Also, by using SMC for the LLC resonant converter ZVS capability can be achieved for no load to full load range, low switching loss,

the highest efficiency at both of high switching frequency. Due to ZVS operation at two specific switching, high frequencies lead to reduce the size of EMI filter.

The paper is organized as follows: In Section 2, the dynamic model for LLC Resonant Converter as battery charger is presented. The design of sliding mode controller for LLC resonant converter is explained in Section 3. The ZVS operation under fixed two switching frequency and Simulated results are discussed in Section 4. Experimental results are presented in Section 5.

II. BATTERY CHARGER

The life and capacity of EV batteries depend on several factors, such as cycle count, charge mode, maintenance, temperature and age. Among these factors, the charge mode has a significant impact on battery life and capacity. EV batteries should be charged with current and voltage levels with low ripple. In addition, the basic requirements for battery chargers are small size and high efficiency, which can be achieved using soft switching techniques. To reduce the switching losses that result from high-frequency operation, resonant power conversion can be used.

A. The LLC Resonant Converter

Half bridge LLC resonant dc-dc converter includes two power switch (Q1, Q2), resonant tank (Lr, Cr, Lm), high frequency electromagnetic transformer, and half-bridge rectifier circuit. The half-bridge circuit of LLC resonant converter is shown in Fig .3.

B. Dynamic Model of The LLC Resonant Converter

Assuming the circuit components is ideal. The circuit behavior can be described as following state space nonlinear Equs. (1)-(5):

$$X = [X_1X_2X_3X_4] = [i_r i_m v_{Cr} v_{Co}], v_{ab} = u, y = X_4 \quad (1)$$

$$\dot{X}_1 = -\frac{1}{L_r} sgn\,(X_1 - X_2).nX_4 - \frac{1}{L_r}X_3 + \frac{1}{L_r}u \quad (2)$$

$$\dot{X}_2 = \frac{1}{L_m} sgn\,(X_1 - X_2).nX_4 \quad (3)$$

$$\dot{X}_3 = \frac{1}{C_r}X_1 \quad (4)$$

$$\dot{X}_4 = \frac{1}{C_o} abs(X_1 - X_4) - \frac{1}{C_o R_o}X_4 \quad (5)$$

Where V_{ab} is the input voltage of the resonant tank, i_r resonant inductance current, i_m is magnetizing inductance current, v_{Cr} is resonant capacitor voltage, V_{Co} output capacitor voltage, and n is the transformer primary-secondary turns ratio.

C. AC Equivalent Circuit of The LLC Resonant Converter

In Fig. 4, AC equivalent circuit of the LLC resonant converter circuit is shown by the first harmonic approximation.

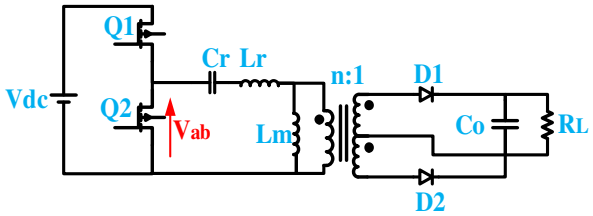


Fig. 3. Typical battery charging power architecture.

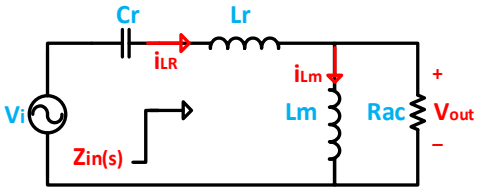


Fig. 4. AC equivalent circuit of the LLC resonant converter.

All elements of the secondary impedances referred to the primary side and secondary side of the transformer turns ratio is multiplied by the square. Input dc voltage and the primary side switching keys took a square waveform. By using the Fourier transform and considering the harmonics of a square wave, Resonant tank input voltage can be considered as a sine wave.

Calculate of ac load resistance:

$$R_{ac} = \frac{8}{\pi^2}\frac{V^2_{out}}{P_{out}} \quad (6)$$

Is achieved with:

$$Z_{in}(s) = \frac{1}{C_r S} + L_r S + \frac{n^2 R_{ac} L_m S}{n^2 R_{ac} + L_m S} \quad (7)$$

Is calculated as:

$$H_{ac}(S) = \frac{V_o}{V_i} = \frac{n^2 R_{ac} L_m S}{n(n^2 R_{ac} + L_m S) Z_{in}(s)} \quad (8)$$

$$V_i = \frac{\sqrt{2}}{\pi}V_{in}\,, V_o = \frac{\sqrt{2}}{\pi}V_{out}\,, H_{dc} = \frac{V_{out}}{V_{in}} \quad (9)$$

The dc transfer function of the resonant converter versus the voltage gain of its ac equivalent circuit can be expressed as follows:

$$H_{dc} = \frac{1}{2}H_{ac} \quad (10)$$

The normalized dc input and output voltages, respectively, are defined as follows:

$$V_{in-N} = \frac{V_{in}}{V_{in-norm}}\,, V_{out-N} = \frac{V_{out}}{V_{out-norm}} \quad (11)$$

$$V_{in-norm} = \frac{V_{in-max} + V_{in-min}}{2} \quad (12)$$

By defining the parameters of K, Q and f_n LLC resonant converter output voltage will be achieved according to Equ.

(1), [8].

$$K = \frac{L_m}{L_r}, Q = \frac{\sqrt{L_r}}{\sqrt{C_r}.R_{ac}} \quad (13)$$

$$V_{out-N}(Q,K,f_n) = \frac{V_{in-N}}{\sqrt{\left(1+\frac{1}{K}+\frac{1}{Kf^2_n}\right)^2+\left(\frac{1}{K}\right)^2.\left(f_n-\frac{1}{f_n}\right)^2}} \quad (14)$$

The steady-state output voltage can be obtained by according to Equ. (14), the normalized dc voltage gain curves are obtained, as shown in Fig. 5, adjusting of the output voltage and load current are achieved by changing the switching frequency between two fixed values.

III. DESIGN CONTROLLER

The first harmonic method is good only near resonant frequency. Fig. 6 shows the block diagram of the proposed controller. The first step is determine the sliding surface in SMC. Generally, the most commonly used sliding surface is a linear combination of system variables. The switching function is obtained by sampling the output voltage and the output capacitor current.

$$S(x,t) = K_v x(t) + K_{ic} i_c(t) + K_P \int x(t) \quad (15)$$

Where x(t) is the output voltage error, x(t) = $x_4(t)$= $v_o(t)$-V_{ref} K_v and K_i are the control gain parameters. The control law is obtained by applying the often-used reaching condition Equ. (22).

$$S.\dot{S} < 0 \quad (16)$$

$$\dot{X} = \frac{1}{C_o} abs(X_1 - X_2) - \frac{1}{C_o R_o} X + u_{eq} \quad (17)$$

$$U = u_{eq} = \begin{cases} 0 & for\ S > 0 \\ 1 & for\ S < 0 \end{cases} \quad (18)$$

Geometrically, the control equivalent can be constructed as:

$$u_{eq} = (1-\alpha).u_+ + \alpha.u_- \quad (19)$$

$$\alpha = -k.sgn(S),\ u_- = f_{sw,min}, u_+ = f_{sw,max} \quad (20)$$

$$f_+ = [\dot{x}, f+u_+], f_- = [\dot{x}, f+u_-], f_{eq} = [\dot{x}, f+u_{eq}] \quad (21)$$

As a convex combination of the values of u on both sides of the surface S(t), the value of α can again be obtained formally from Equ. (20). It is correspond to requiring that the system trajectories be tangent to the surface. This intuitive construction is summarized in Fig. 7, where f is the switching frequency.

$$U = \begin{cases} 0 & for\ S > \sigma \quad or\ (|S| < \sigma, \dot{S} < 0) \\ 1 & for\ S < -\sigma \quad or\ (|S| < \sigma, \dot{S} > 0) \end{cases} \quad (22)$$

In (26), σ is the phase delay and ξ is the boundary layer width on the phase plane. In the proposed controller, three cirquit

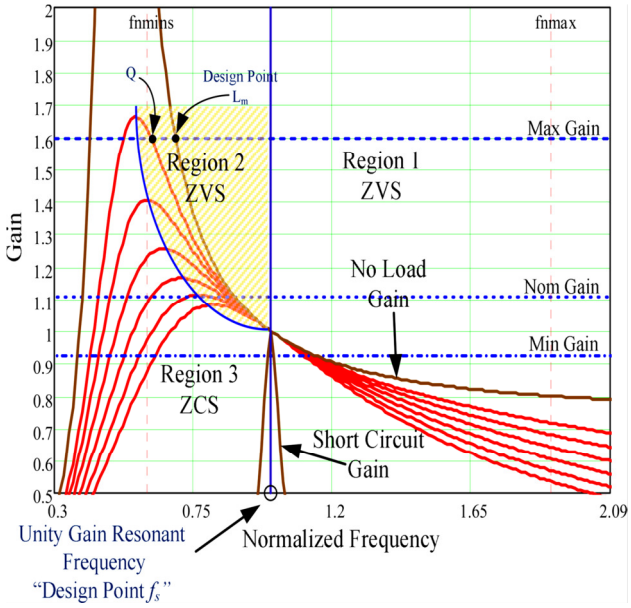


Fig. 5. Normalized dc voltage gain curves [20]

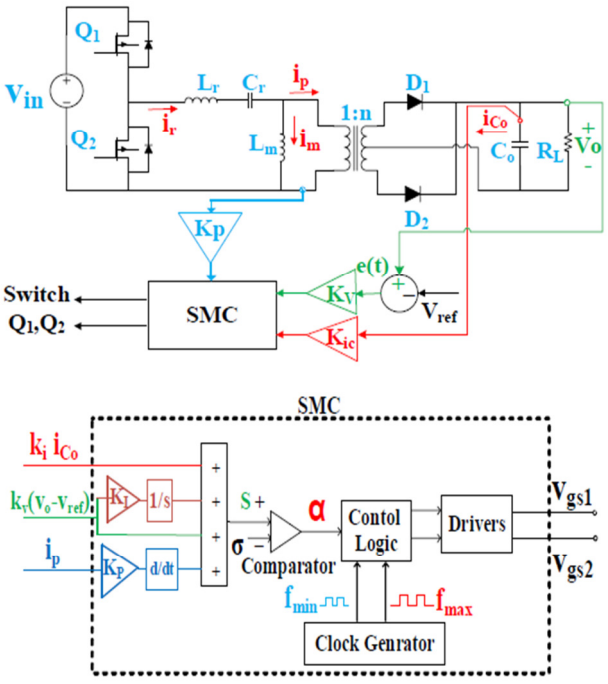


Fig. 6. Proposed sliding-mode control scheme for LLC resonant converter

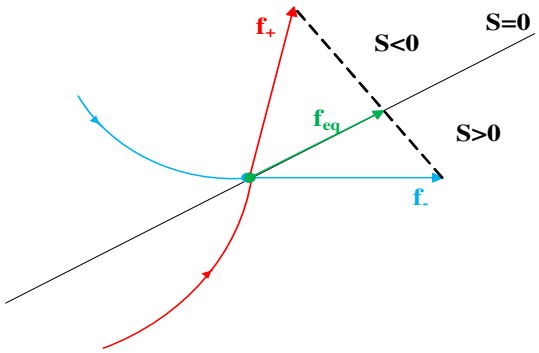


Fig. 7. Filippov's construction of the equivalent dynamics in sliding mode [21]

control parameters (K_v, K_i and ξ) are involved. According to the relationships between them, these parameters can be simplified into two control parameters:

$$K = \frac{K_v}{K_{ic}.C_o}, \sigma = \frac{\xi}{K_{ic}.C_o} \quad (23)$$

One of the sliding mode controller is chattering phenomenon. To overcome this problem, a thin boundary layer is considered neighbor the switching surface.

$$B(t) = \{X, |S(X,t) \leq \varphi|\}, \xi = \frac{\varphi}{\lambda^{n-1}} \quad (24)$$

Where φ is the boundary layer thickness and λ is strictly positive constant. Fig. 8, shows sliding surface with boundary layer in phase plane.

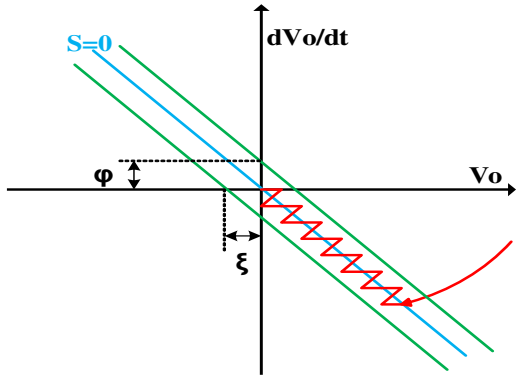


Fig. 8. Sliding surface with boundary layer in phase plane

IV. SIMULATION RESULT

Fig. 9, shows the steady-state simulation waveforms of voltage across MOSFET Q_2, resonant tank current i_{Lr} and resonant capacitor voltage V_{Cr}. The operation of LLC resonant converter with sliding mode controller in two mode is shown in Fig. 10, below resonant frequency mode and above resonant frequency mode, the minimum switching frequency is selected by the constant value, if the amplitude of the control signal U is positive. At the same time it is applied to the MOSFET gate that it is illustrated VQ2-a in Fig .10, The converter is operated in below resonant frequency mode in this state. The maximum switching frequency is selected by the constant value if the amplitude of control signal U reaches to zero. At the same time it is applied to the MOSFET gate. Fig. 10, shows the proper time-delay, minimum switching frequency and maximum switching frequency values to achieve the ZVS operation are three important subjects that must be realized, for reducing the generated EMI noise and improving the efficiency and performance of the converter. To illustrate the strong robustness against parametric uncertainties and the fast transient response of the proposed sliding mode control strategy, uncertainties is applied to resonant tank parameters.

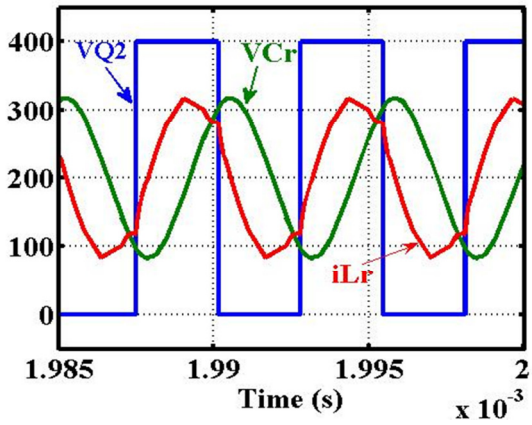


Fig. 9. Steady-state simulation waveforms of output voltage Q2, resonant tank current i_{Lr}, and resonant capacitor voltage (input voltage: 360V, output voltage: 48V, I_O: 8A)

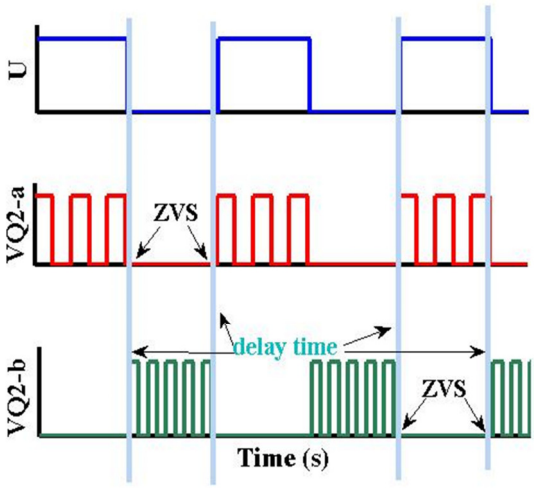


Fig. 10. Schematic diagram of zero-crossing switch Sliding mode control signal U, voltage across MOSFET Q_2 at minimum frequency (V_{Q2}-a) and maximum frequency (V_{Q2}-b)

In Fig .11, at t=0.07 s, 15 percent is applied to resonant inductance L_r, then at t=0.1s 5 percent is applied to electromagnetic transformer inductance L_m, finally, at

t=0.13s, 15 percent is applied to resonant capacitor C_r. According to Fig. 11, by considering uncertainties in resonant tank parameters, SMC has more faster convergence time under the condition uncertainties in resonant tank parameters.

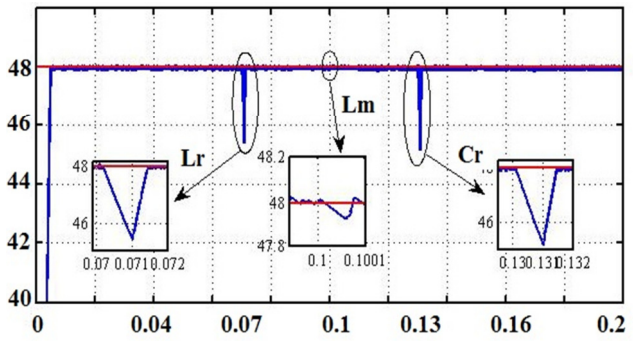


Fig. 11. uncertainties in the parameters of resonant tank

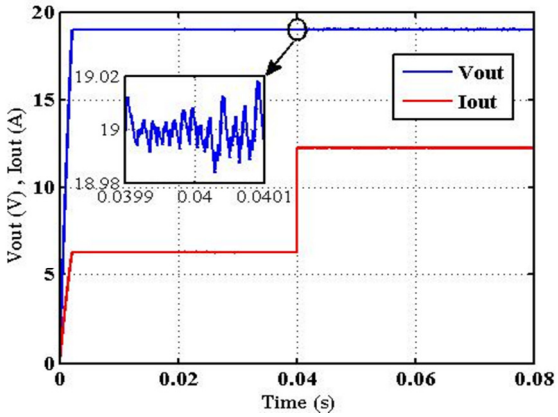


Fig. 12. Dynamic response of the output voltage in the presence load variations 6 A to 12 A

Also, SMC is able to regulate the output voltage less than 1ms with uncertainties conditions. The dynamic response of the output voltage in the presence load variations is shown in Fig. 12. According to results, the SMC is able to regulate the output voltage to its desired value under the load variation from 6A to 12A. As seen response convergence to variation is less than 100µs and overshoot is less than 2mv.

V. BATTERY CHARGER

A prototype is implemented to verify the performance of the battery charger based half-bridge LLC resonant converter, as shown in Fig. The LLC resonant converter specification and designed parameters are shown in Tables I and II. The proposed sliding-mode controller has been implemented following the scheme shown in Fig. 14. It shows waveforms of sliding mode control signal U and switching frequency of sliding mode control signal U and switching frequency. The results illustrate that switching frequency is selected according to the sliding-mode control signal U. As can be seen from Fig. 14, when amplitude of the control signal U reaches a value of 1, the minimum switching frequency (f_s-min) is selected and switching frequency lower than resonant frequency ($f_s < f_r$). Then the maximum switching frequency is selected when the control signal U becomes zero and the switching frequency upper than resonant frequency ($f_s > f_r$). Fig. 15 shows the experimental waveforms of the resonant tank current and voltage across bottom MOSFET under full load 11A output current and 300V input voltage. The waveforms of output voltage and ripple output voltage are shown in Fig 16. Fig 17 shows four distinct operating modes: bulk, absorption, equalization and maintenance. In the bulk mode, the time between 0-30 min, battery voltage increases from 36V to 60V, and this mode the minimum battery current is 11A.

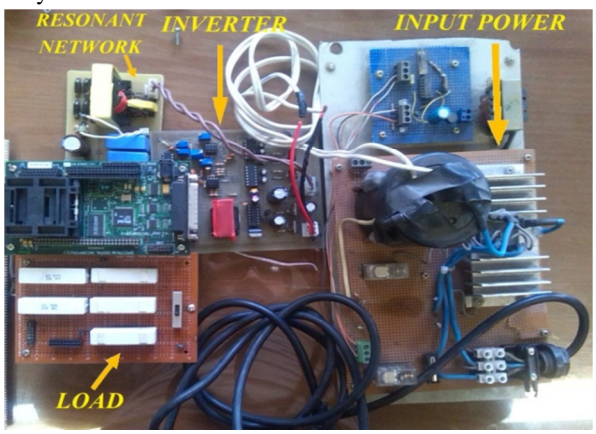


Fig. 13. Photo of the prototype *LLC* resonant convert

Table I. Parameters OF LLC resonant converter

Symbol	Parameter	Value / Unit
V_{in}	Input voltage	300-420 v
V_{out}	Output voltage	36-72 v
L_r	Resonant inductance	101.5 µH
L_m	Magnetizing inductance	105 µH
C_r	Resonant capacitor	6.7 µF
C_o	Output capacitor	1000 µF
f_r	Resonant frequency	150 KHZ
f_{min}	Low frequency	135 KHZ
f_{max}	High frequency	200 KHZ
n	Transformer ratio	40:4
k_v	Voltage gain	0.8
k_{ic}	Current capacitor gain	$9.6*10^{-4}$
k_m	Current primary gain	$2.67*10^{-4}$
k_i	Integral gain	300
λ	positive constant	20
σ	Phase delay	500
T_D	Dead time	400 ns

Table II. Components used in the prototype converter

Symbol	Parameter	Value / Unit
Q	MOSFET	IRFZ44N
D	Diode	HER308
C_r	Resonant Capacitor	6.7 nF
L_m	Resonant Inductor	40-100 µH
L_r	Magnetizing Capacitor	484 µH
C_O	Output Capacitor	2000 µH, 100V
DSP	Controller	TMS320LF24070A
Q	MOSFET	IRF740P
D	Diode	HER308

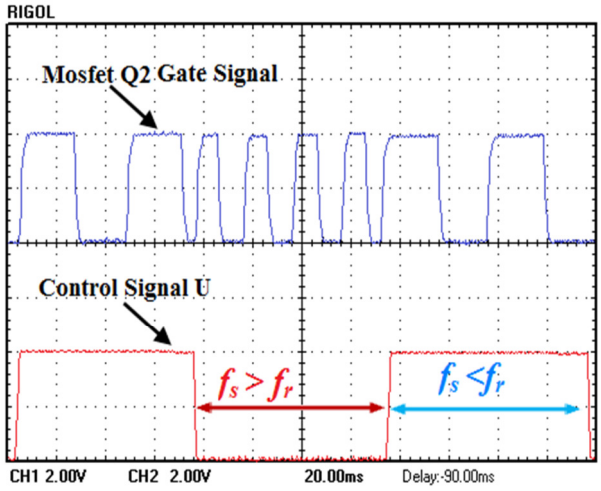


Fig. 14. Switching frequency and sliding-mode control signal U

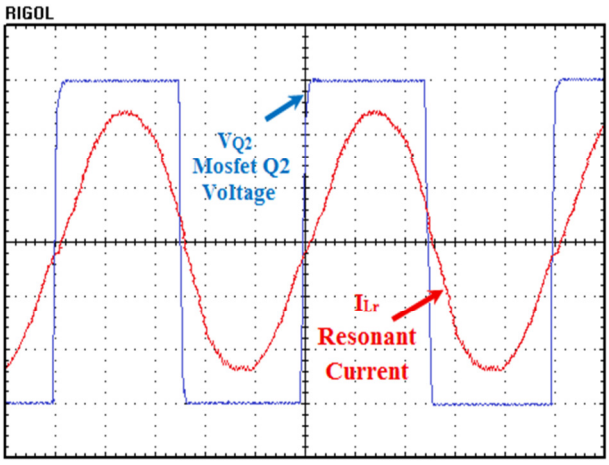


Fig. 15. Resonant tank current (I_{Lr}) and voltage across MOSFET Q_2 (V_{Q2}) at V_O= 48 V, I_O=8 A, and f_s=150 kHz (Y-axis: Ch1=V_{Q2} 100 V/div, Ch2= I_{Lr} 2 A/div. X-axis: 1 µs/div).

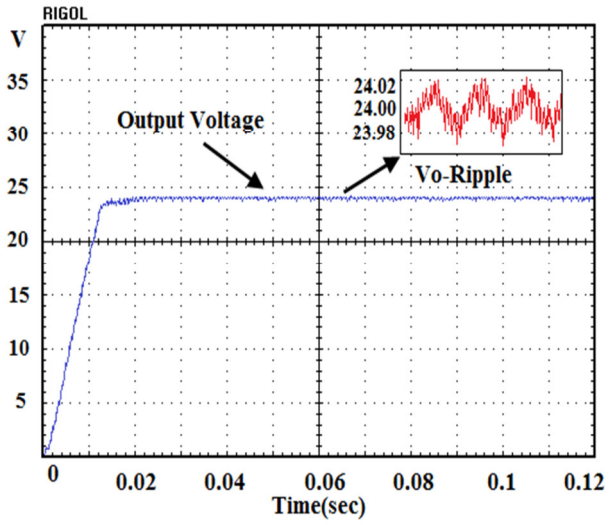


Fig. 16. Output voltage V_O and Output voltage ripple ($V_{O\text{-}Ripple}$) at V_O= 24 V

In absorption mode, the time between 30-70 min, battery voltage charging remains constant and the battery current value is greatly reduced from 11A to 3.3A. In equalization mode, at the time between 70-95 min battery voltage increases up to a maximum value of 72V, this mode is ends when the voltage and current reach to constant amount and this moment battery charge is 100%. In the maintenance mode, the time between 30-70 min, battery voltage reaches to 48V and the charger only supplies limited current to offset the internal soft discharge. The efficiency LLC resonant converter for battery charging of EV for various amount of K are given in Fig. 18, as can be seen the maximum efficiency of 96% LLC resonant battery at full load conditions is obtained at the voltage of 72V.

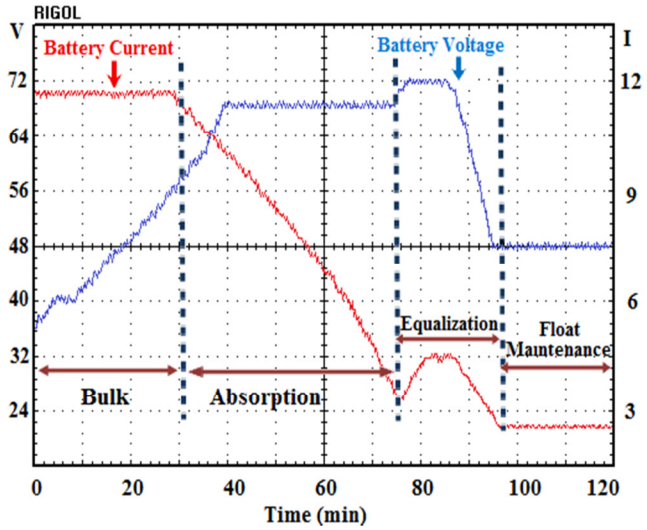


Fig. 17. Battery voltage and current in during charging time

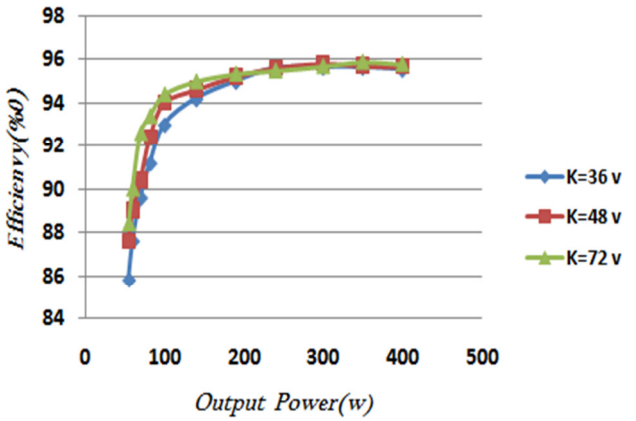


Fig.18. LLC resonant converter efficiency under different voltages

VI. CONCLUSION

In this paper, sliding mode control for the LLC resonant converter in battery charger for electric vehicles is designed and implemented. Due to robustness of control strategies against uncertainties and less electromagnetic interference, a desirable transient response to changes in input voltage, output voltage and load current are obtained. Also, the eliminates of both low- and high-frequency current ripple on the battery, maximizes the battery life without penalizing the volume of the charger. Proposed method has a wide range of input voltage, output voltage, and load current changes. The input voltage is changed between 300-420 V, output voltage is changed between 36-72 V, and load current is changed 0-11 A. Finally, the efficiency of proposed method is 96 %.

REFERENCES

[1] G. Cao, W. Dou, K, Sun, Y, Wang "Design Optimization of LLC Converter for Battery Charger with Wide Output Voltage Range," *2018 IEEE 27th International Symposium on Industrial Electronics (ISIE)*, pp. 1182 – 1187.

[2] D. Gumera, A. Caberos, Sh. Huang, "Design and Implementation of a High Efficiency Cost Effective EV Charger Using LLC Resonant Converter," *2017 Asian Conference on Energy, Power and Transportation Electrification (ACEPT)*.

[3] F. Musavi, M. Craciun, D. S. Gautam, W. Eberle and W. D. Dunford, "An *LLC* Resonant DC–DC Converter for Wide Output Voltage Range Battery Charging Applications," *IEEE Trans. Power Electron.*, vol. 28, no. 12, pp. 5437–5445, December 2013.

[4] A. Emadi, S. Williamson, and A. Khaligh, "Power electronics intensive solutions for advanced electric, hybrid electric, and fuel cell vehicular power systems," *IEEE Trans. Power Electron.*, vol. 21, no. 3, pp. 567– 577, May 2006.

[5] A. M. Rahimi, "A lithium-ion battery charger for charging up to eight cells," in *Proc. IEEE Conf. Vehicle Power Propulsion*, 2005, pp. 131–136.

[6] B . Singh, B. N. Singh, A. Chandra, K. Al-Haddad, A. Pandey, and D. P. Kothari, "A review of single-phase improved power quality AC-DC converters," *IEEE Trans. Ind. Electron.*, vol. 50, no. 5, pp. 962–981, Oct. 2003.

[7] L. Petersen and M. Andersen, "Two-stage power factor corrected power supplies: The low component-stress approach," in *Proc. IEEE Appl. Power Electron. Conf. Expo.*, 2002, vol. 2, pp. 1195–1201.

[8] L. Yang, B. Lu, W. Dong, Z. Lu, M. Xu, F. C. Lee, and W. G. Odendaal, "Modeling and characterization of a 1KW CCM PFC converter for conducted EMI prediction," in *Proc. IEEE Appl. Power Electron. Conf. Expo.*, 2004, vol. 2, pp. 763–769.

[9] R. Beiranvand, B. Rashidian, M. R. Zolghadri, and S. M. . Alavi, "Using LLC Resonant Converter for Designing Wide-Range Voltage Source," *IEEE Trans. Power Electron.*, VOL. 58, NO. 5, pp. 1746–1756, MAY 2011.

[10] S. Chudjuarjeen, A. Sangswang, and C. Koompai, "An improved LLC resonant inverter for induction-heating applications with asymmetrical control," *IEEE Trans. Ind. Electron.*, vol. 58, no. 7, pp. 2915–2925, Jul. 2011.

[11] J.-Y. Lee, Y.-S. Jeong, and B.-M. Han, "An isolated DC/DC converter using high-frequency unregulated LLC resonant converter for fuel cell applications," *IEEE Trans. Ind. Electron.*, vol. 58, no. 7, pp. 2926–2934, Jul. 2011.

[12] Y. C. Chuang, Y. L. Ke, H. S. Chuang, and Y. M. Chen, "Analysis and im plementation of half-bridge series–parallel resonant converter for battery chargers," *IEEE Trans. Ind. Appl.*, vol. 47, no. 1, pp. 258–270, Feb. 2011.

[13] R. Beiranvand, B. Rashidian, M. R. Zolghadri, and S. M. H. Alavi, "Optimizing the normalized dead-time and maximum switching frequency of a wide-adjustable-range LLC resonant converter," *IEEE Trans. Power Electron.*, vol. 26, no. 2, pp. 462–472, Feb. 2011.

[14] R. Beiranvand, B. Rashidian, M. R. Zolghadri, and S. M. H. Alavi, "A design procedure for optimizing the LLC resonant converter as a wide output range voltage source," *IEEE Trans. Power Electron.*, vol. 27, no. 8,pp. 3749–3763, Aug. 2012.

[15] A. Ghasemian, A. Taheri, "Constrained Near Time-Optimal Sliding Mode Control of Boost Converters Based on Switched Affine Model Analysis," *IEEE Trans. Power Electron.*, vol. 65, no. 1,pp. 887–897, 2018.

[16] S.N. Mirebrahimi, F. Merrikh-Bayat, A, Taheri, "Voltage-Mode Robust Controller Design for DC-DC Boost Converter at the Presence of Wide Load and Input Voltage Variations Based on Finite-State-Machine Model, " *IET Power Electronics*., Vol. 11 , no. 5 , pp. 866 – 875, April 2018.

[17] G. Ivensky, S. Bronshtein, and A. Abramovitz, "Approximate analysis of resonant LLC DC-DC converter," *IEEE Trans. Power Electron.*, vol. 26, no. 11, pp. 3274–3284, Nov. 2011.

[18] Y. yuan, F. Jeng, "Robust Nonsingular Terminal Sliding

Mode Control for Nonlinear Magnetic Bearing System,"*IEEE Trans. Control Systems Technology*, 2011. 19(3): pp. 636-643.

[19] J. Minjae, K. Hosung, and B. Joowon, "Dynamic analysis and optimal design of high efficiency full bridge LLC resonant converter for server power system," in *Applied Power Electronics Conference and Exposition (APEC),* 2012. pp. 1292- 1297.

[20] S. Geng, Y. Zhao, Sh. Sun, X. Wu, Y. Zheng and J. Liu, "Sliding Mode Control of LLC Resonant DC-DC Converters," *in IEEE 25th International Symposium on Industrial Electronics (ISIE)*, 2016, pp. 1034–1037.

[21] J.J. ESlotine (1991); Applied Nonlinear Control:New Jersi, 1,Jennifer Wenzel.ISBN-0-13-040890-5.1991.

[22] S. Geng, Y. Zhao, Sh. Sun, X. Wu, Y. Zheng and J. Liu, "Sliding Mode Control of LLC Resonant DC-DC Converters," *in IEEE 25th International Symposium on Industrial Electronics (ISIE)*, 2016, pp. 1034–1037.



Asghar Taheri . Was born in Zanjan, Iran. He received Ph.D degree in electrical engineering from Iran University of Science and Technology. He is currently an Associate Professor in the department of Electrical Engineering University of Zanjan, Zanjan, Iran. His current research interests include AC motor control, DC-DC converters, and PWM converter/inverter systems.



Nader Asgari was born in Zanjan, Iran. He received his B.S. degree in Electrical Engineering from the University of Zanjan, Zanjan, Iran, in 2010, and his M.S. degrees in Electrical Engineering from the University of Zanjan, Zanjan, Iran, in 2015. He is currently Electrical Engineer at Andishe-Negar-e-Pars company. His current research interests include renewable energy, DC-DC converter control and charger battery for electric vehicles.

IECO

This page intentionally left blank.